Surface impedance of $YBa_2Cu_3O_7/Y_{0.6}Pr_{0.4}Ba_2Cu_3O_7$ bilayers: Possible evidence for the proximity effect

Michael S. Pambianchi,* C. Kwon, T. Venkatesan, and Steven M. Anlage†
Center for Superconductivity Research, Department of Physics, University of Maryland, College Park, Maryland 20742-4111
(Received 1 August 1996)

Measurements of the surface impedance of superconductor/normal-metal bilayers provide information on the proximity coupling between superconductors with different transition temperatures. Surface impedance data on *c*-axis $YBa_2Cu_3O_{7-\delta}/Y_{0.6}Pr_{0.4}Ba_2Cu_3O_7$ bilayers is consistent with either proximity coupling in the *c* direction between the two materials with a very weak proximity-induced condensate and/or the behavior of two isolated superconductors in a bilayer geometry. At least one of the characteristics of proximity coupled superconductors, namely, a strong downturn of the effective penetration depth above the lower of the two transition temperatures, was not observed in the *c*-axis high-T_c bilayer films studied. However, the increase of the surface resistance above the T_c of the Pr-doped layer is a sign that the conductivity of the $Y_{0.6}Pr_{0.4}Ba_2Cu_3O_7$ layer is strongly enhanced above its T_c, in agreement with THz spectroscopy measurements. [S0163-1829(96)03645-4]

I. INTRODUCTION

Although the superconducting proximity effect has been amply demonstrated in low-T_c superconductor/normal-metal bilayer systems, there is little evidence of this effect in high-T_c cuprate superconductors. Reasons for this lack of evidence may be related to the same materials issues which originally plagued the low-T_c superconductors, namely, interdiffusion and alloy formation of the two layers or insulating barriers at the interface.[1] However, the cuprate superconductors have additional intrinsic features which may make the proximity effect more difficult to observe. These include the highly two-dimensional nature and short coherence lengths of these materials. The latter feature makes the cuprates particularly sensitive to the effects of doping disorder, as relatively small regions which are overdoped or underdoped have electrical and superconducting properties which are significantly different from the optimally doped regions. In addition, exotic order parameter symmetries may alter the character of proximity coupling in the cuprates.[2,3]

The bulk of the evidence for proximity coupling in the cuprates has come from study of the critical current of superconductor/normal-metal/superconductor (*S*-*N*-*S*) junction devices[4] as a function of *N*-layer thickness[5–7] and temperature.[1,5,7] Because *N*-layer thicknesses are only 10–100 nm in such studies, junction properties can be strongly influenced by compositional inhomogeneity.[7–9] Thus, these experiments provide no definitive evidence for the proximity effect in the cuprates.

A separate question regards whether or not proximity coupling exists for current flow in the *c* direction in the cuprates. Deutscher has argued that if the *c*-axis conduction process is nonmetallic, there should be no induced order parameter in a normal metal in the *c* direction.[10] Hence the existence or absence of proximity coupling in the *c* direction is directly related to the nature of *c*-axis transport in the cuprates.

The existence and nature of proximity coupling in the cuprates are therefore not clear. In fact, the more basic question of whether or not the doped cuprates are in the clean or dirty limit is also unclear.[11] Our objective in this work is to introduce a method of investigating the proximity effect in cuprate superconductors. As with transport measurements in *S*-*N*-*S* devices, this method is susceptible to the problem of dopant disorder. However, it does not rely on building submicrometer barriers or trilayer devices to detect the proximity effect. Our method is to simply measure the microwave surface impedance of *S*/*N* bilayer films. This technique has proved to be quite successful for quantifying the proximity effect in low-T_c proximity coupled systems such as Nb/Al, Nb/Cu,[12–14] and $Mo_{80}Ge_{20}$/Ag.[15] As we shall see, this technique also gives insight into the normal state electrodynamic properties of the lower-T_c film.

II. SAMPLES AND EXPERIMENT

It is believed that the best prospect for identifying the proximity effect in the cuprates is to use a doped cuprate with a suppressed T_c as the normal metal layer.[1,16] Noble metals in contact with the cuprates have a large mismatch in Fermi velocities and density of states at the Fermi energy, and should result in poor proximity coupling.[17] Clearly, good lattice match and thermal expansion match are required for optimal electrical contact to the cuprates.[1] Hence the best prospects for observing the proximity effect in the cuprates are with a doped material with reduced T_c, but with similar crystallographic properties. A convenient dopant for suppressing T_c is Pr substituted for Y in $YBa_2Cu_3O_{7-\delta}$ (YBCO). A bilayer of YBCO and Pr-doped YBCO is particularly attractive because it has been demonstrated that the length scale for interdiffusion of YBCO and Pr-doped YBCO is less than one unit cell.[18]

The samples used in this experiment are thin films of YBCO, $Y_{0.6}Pr_{0.4}Ba_2Cu_3O_{7-\delta}$ (YPrBCO), and bilayer YBCO/YPrBCO films, all prepared by pulsed laser ablation on $LaAlO_3$ substrates. The 3000-Å-thick *c*-axis YBCO films have an ac susceptibility transition temperature of $T_c = 90.0$ K with a 10%–90% transition width of approximately 0.5

K.[19,20] The 3000-Å-thick c-axis YPrBCO films were also grown by pulsed laser deposition on $LaAlO_3$ substrates, and have an ac susceptibility transition temperature of $T_{cN}=57.5$ K, with a 10%–90% transition width of approximately 0.5 K.[21] The 3000-Å-thick c-axis YBCO/variable-thickness c-axis YPrBCO bilayer films were grown sequentially *in situ* to prevent degradation of the interface. The YBCO/YPrBCO bilayers were made with YPrBCO thicknesses of 0, 1000, 2000, and 3000 Å, all with a YBCO base layer 3000 Å thick.

The experiments were performed by making parallel plate transmission line microwave resonators out of the thin films.[22] Two rectangular congruent films are separated by a Teflon sheet, $d=25$, 50, or 75 μm thick, forming a resonant length of superconducting parallel plate transmission line in two dimensions. The lowest-order modes (10) and (01) were used for the present measurements and both resonate in the vicinity of 11 GHz. The change in magnetic penetration depth is obtained from the frequency shift of the resonator with temperature, $f_0(T)$, while the absolute surface resistance is obtained from the quality factor $Q(T)$ of the resonance.[22–24] The surface resistance is estimated from $R_s(T) \leqslant \pi \mu_0 f_0 d/Q$, while the change in the effective penetration depth is obtained from $\Delta\lambda_{\rm eff}(T)=(d/2)\{[f_0(T_0)/f_0(T)]^2-1\}$, where d is the dielectric thickness and T_0 is the minimum temperature achieved in the experiment.[25] Further details of the conversion of the raw frequency shift and quality factor data into $\Delta\lambda(T)$ and $R_s(T)$ are contained in other publications.[12,13,26]

First, single-layer YBCO films were measured by this technique. It was found that after the contributions of dielectric and radiation loss were subtracted, the surface resistance of these films was less than 6 $\mu\Omega$ at 11.9 GHz and 4.2 K.[24] This value of the surface resistance is as low as one can reliably measure with the parallel plate resonator technique.[22] The single-layer YPrBCO films were also measured as a pair. Data on the YBCO/YPrBCO bilayer films were obtained using one (much less lossy) single-layer YBCO film and one bilayer film; the frequency shift and surface resistance for the single-layer YBCO were subtracted from the composite data to get the change in penetration depth and absolute surface resistance of the YBCO/YPrBCO bilayer film alone. Note that in the bilayer films, the YBCO layer is deposited directly on the substrate, while the YPrBCO layer is grown on the YBCO and is directly exposed to the microwave electric and magnetic fields.

III. DATA

Surface impedance data on the single-layer YBCO and YPrBCO films are shown in Fig. 1. The temperature dependence of $\Delta\lambda_{\rm eff}(T)$ for the single-layer 3000-Å-thick YBCO film could be fit to the empirical form[27] $\lambda(T)=\lambda(0)/[1-(T/T_c)^2]^{1/2}$ over the temperature range 4.2 K $<T<$ 81.5 K, with $\lambda(0)=2200$ Å and $T_c=83.8$ K used as fitting parameters. The single-layer YBCO films have a surface resistance of 920 $\mu\Omega$ at 77 K, 11 GHz and less than 10 $\mu\Omega$ at 4.2 K, 11 GHz (Fig. 1).

The single-layer 3000-Å-thick YPrBCO films have a surface resistance of approximately 600 $\mu\Omega$ at 40 K, 11 GHz. The temperature dependence of $\Delta\lambda_{\rm eff}(T)$ could be fit to the

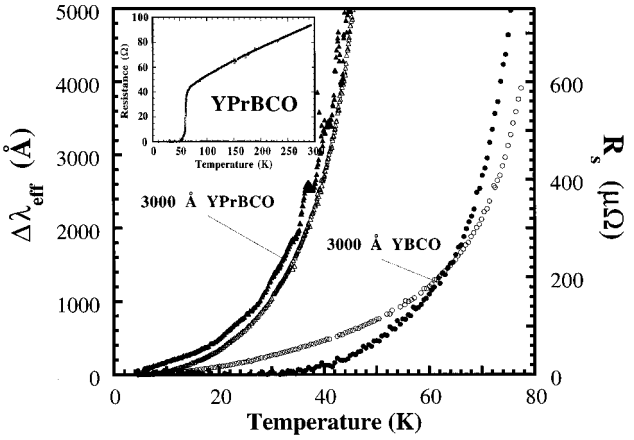

FIG. 1. Change in effective penetration depth (open symbols) and surface resistance (solid symbols) as a function of temperature for single layer YBCO and YPrBCO thin films. Inset shows the dc resistance versus temperature for the YPrBCO film.

empirical form[27] $\lambda(T)=\lambda(0)/[1-(T/T_c)^2]^{1/2}$ over the temperature range 5.5 K $<T<$ 45.8 K, with $\lambda_{\rm eff}(0)=4925$ Å [giving $\lambda(0)=3450$ Å using standard thin film corrections[24,28]] and $T_c=52.4$ K. However, $\Delta\lambda_{\rm eff}(T)$ increases rather gradually at low temperatures compared to the YBCO film, so that the quality of this fit is not as good as that for the YBCO film.

The change in effective penetration depth and surface resistance of the YBCO/YPrBCO bilayer films are shown in Figs. 2 and 3, respectively. Note that the bilayers show a kink in $\Delta\lambda_{\rm eff}(T)$ (Fig. 2) at a temperature in the vicinity of T_{cN}. The kink becomes more distinct with increasing thickness of the YPrBCO layer. There is also a clear nonmonotonic behavior of the effective surface resistance of the bilayers (Fig. 3). The surface resistance[25] shows a minimum at a temperature $T_{\rm min}$ above T_{cN}, then rises to a maximum value several kelvin below T_{cN} at $T_{\rm max}$, and then drops back down (these temperatures are tabulated in Table I). Note that the bump width, as defined by the separation in temperature between the minimum and maximum R_s values, increases

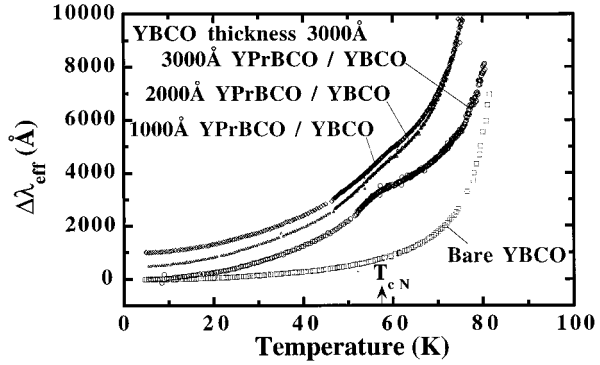

FIG. 2. Change in effective magnetic penetration depth $\Delta\lambda_{\rm eff}(T)$ for a 3000-Å-thick YBCO film, and YBCO/YPrBCO bilayers each with a 3000-Å-thick YBCO base layer and YPrBCO layers of 1000 Å (offset vertically 1000 Å), 2000 Å (offset vertically 500 Å), and 3000 Å.

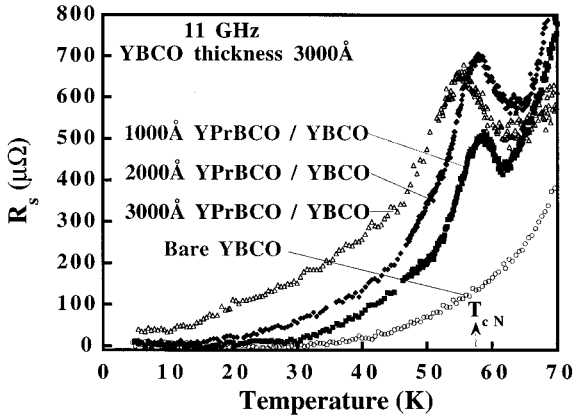

FIG. 3. Surface resistance $R_s(T)$ at 11 GHz for a 3000-Å-thick YBCO film, and YBCO/YPrBCO bilayers each with a 3000-Å-thick YBCO base layer and YPrBCO layers of 1000, 2000, and 3000 Å.

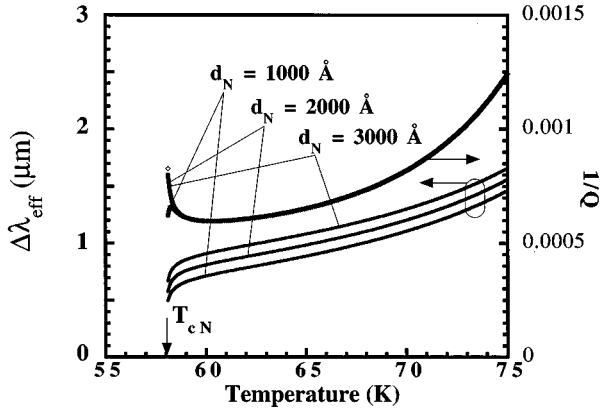

FIG. 4. Calculated change in effective penetration depth $\Delta\lambda_{\rm eff}(T)$ and surface resistance (proportional to $1/Q$) in the proximity electrodynamics model using estimated ab-plane transport properties for the YBCO and YPrBCO layers.

with increasing YPrBCO layer thickness, and that the resistance maximum temperature monotonically decreases with increasing YPrBCO thickness. It should also be noted that the minima in $R_s(T)$ are all above the T_{cN} values obtained by either fitting to $\Delta\lambda(T)$ of the single-layer YPrBCO or by zero dc resistance measurements.

IV. DISCUSSION

A detailed model of the electrodynamics of proximity-coupled bilayer systems has been developed and applied to low-T_c bilayers.[12–14] In that model, elementary proximity effect physics was combined with superconductor electrodynamics to calculate the frequency shift and quality factor of low-T_c S/N bilayer parallel plate resonators. The model was generally successful at quantitatively describing the outcome of the experiments.[12–14]

In our measurements, rf currents flow parallel to the S/N interface in the bilayer films. However, the microscopic mechanism for the proximity effect involves quasiparticles which have some normal component to the S/N interface. Hence it is not clear whether our measurements should be sensitive to proximity coupling in the ab plane or the c direction. Therefore, we have applied the model to the present measurements for two situations. In both cases, we assume that there is a proximity-induced condensate in the YPrBCO layer for temperatures above T_{cN}. In one case, we use the ab-plane electrodynamic properties to calculate the electron diffusion coefficient and coherence length in the YPrBCO layer, while in the second case we use the c-axis transport properties to determine the YPrBCO coherence length. The ab-plane case has a longer coherence length than the c-axis case; hence the length scale and strength of the proximity-induced condensate are dictated by this choice. In both cases we use the traditional de Gennes–Deutscher theory of proximity electrodynamics.[5,29]

The model calculation for the case of ab-plane proximity coupling is shown in Fig. 4. The parameters used in the calculation for the base superconductor layer are $T_{cs}=90$ K, zero-temperature penetration depth $\lambda_s(0)=2200$ Å, normal state conductivity $\sigma_s=3\times10^6$ $1/\Omega$ m, and thickness $d_s=3000$ Å, while for the normal metal layer $T_{cN}=58$ K, $\lambda_N(0)=3450$ Å, Fermi velocity $v_{FN}=10^5$ m/s, mean free path $\ell_{\rm MFPN}=100$ Å, and normal state conductivity $\sigma_N=2\times10^6$ $1/\Omega$ m. The effective penetration depth (Fig. 4) shows a deep depression beginning approximately 2 K above T_{cN}, while the surface resistance (proportional to $1/Q$) shows a minimum at about the same temperature. The calculation for a 1000-Å-thick YPrBCO layer on YBCO also displays a small peak in $R_s(T)$ just above T_{cN}. However, the measured effective penetration depth (Fig. 2) shows no sign of dropping above T_{cN}, whereas the measured surface resistance does show a minimum above T_{cN} which is qualitatively similar to that of the ab-plane proximity calculation.

The model calculation for the case of c-axis proximity coupling between the YBCO and YPrBCO is shown in Fig. 5. The parameters used in the calculation for the base superconductor layer are $T_{cs}=90$ K, zero-temperature penetration depth $\lambda_s(0)=2200$ Å, normal state conductivity $\sigma_s=3\times10^5$ $1/\Omega$ m, and thickness $d_s=3000$ Å, while for the

TABLE I. Key temperatures in $\Delta\lambda_{\rm eff}(T)$ and $R_s(T)$ data on YBCO/YPrBCO bilayer films, as well as similar features in the two superconductor model calculation.

	Data			Two-superconductor model		
d_N (Å)	$T_{\rm kink}$ in $\Delta\lambda_{\rm eff}(T)$ (K)	$T_{\rm min}$ of $R_s(T)$ (K)	$T_{\rm max}$ of $R_s(T)$ (K)	$T_{\rm kink}$ (K)	$T_{\rm min}$ (K)	$T_{\rm max}$ (K)
1000	–	61.1	59.4	55.8	56.9	55.12
2000	58.5	62.0	58.3	55.8	57.64	53.2
3000	56.5	60.48	55.6	55.8	57.64	52.6

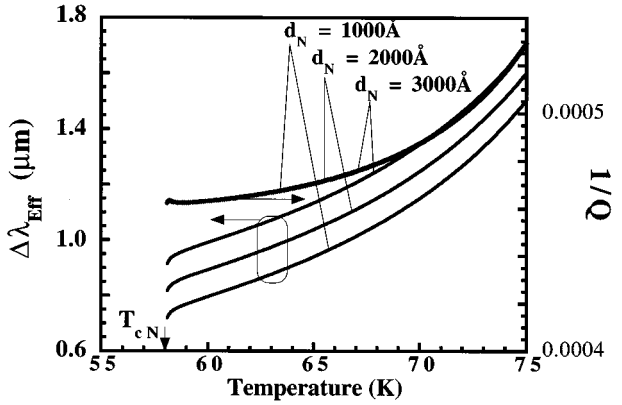

FIG. 5. Calculated change in effective penetration depth $\Delta\lambda_{\mathrm{eff}}(T)$ and surface resistance (proportional to $1/Q$) in the proximity electrodynamics model using estimated c-axis transport properties for the YBCO and YPrBCO layers.

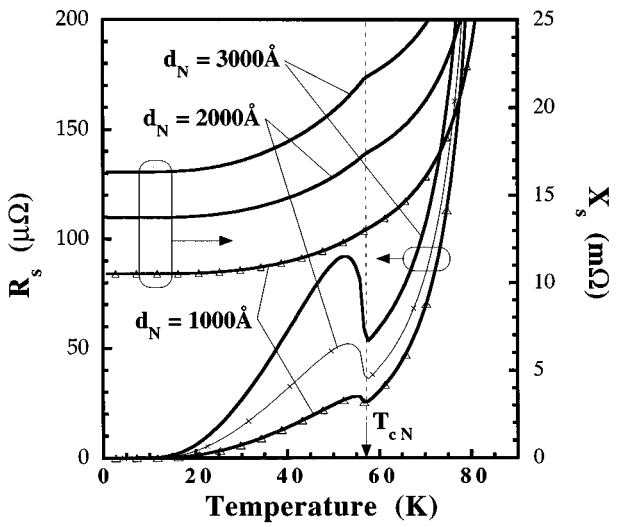

FIG. 6. Calculated surface reactance $X_s(T)$ and surface resistance $R_s(T)$ in the two-superconductor electrodynamics model using estimated ab-plane transport properties for the YBCO and YPrBCO layers.

normal metal layer $T_{cN}=58$ K, $\lambda_N(0)=3450$ Å, Fermi velocity $v_{FN}=10^4$ m/s, mean free path $\ell_{\mathrm{MFPN}}=10$ Å, and normal state conductivity $\sigma_N=2\times10^5$ $1/\Omega$ m. The last three quantities are rough estimates of the c-axis transport properties of YPrBCO. The calculated effective penetration depth (Fig. 5) now shows only a very slight downturn within 1 K of T_{cN}, but the calculated surface resistance now shows no evidence whatsoever of a minimum above T_{cN}. This calculation shows little resemblance to the data in Figs. 2 and 3.

Hence we must conclude that neither type of proximity model can completely explain the observed effective penetration depth and surface resistance data in the YBCO/YPrBCO bilayers. However, an upper bound can be put on the coherence length in YPrBCO in the context of our proximity screening model. The finite measurement resolution for $\Delta\lambda$, as well as the finite transition width of the YPrBCO, put a limit on how small a downturn in $\Delta\lambda(T)$ one can observe above T_{cN}. In addition, there is a fundamental problem arising from the great difference in length scales between the screening length and the coherence length in the normal metal. The proximity-induced superconductivity in the normal metal is expected to occur on a much shorter length scale than the magnetic screening; hence the perturbation of the parallel plate resonator properties due to the proximity effect is correspondingly small. Subject to these constraints, we estimate that $\xi_N(T_{cN}+2\ \mathrm{K})$ must be no greater than about one unit cell, i.e., $\xi_N(T_{cN}+2\ \mathrm{K})\lesssim 1$ nm. This conclusion is consistent with the absence of metallic transport in the c direction in YPrBCO.[10]

An alternative model is simply to suppose that the two layers have no proximity coupling whatsoever, and they act as two independent superconductors with different T_c's in a bilayer geometry. In this two-superconductor model, the upper film has a lower T_c, but both films are assumed to have Mattis-Bardeen electrodynamics below their respective transition temperatures.[30] The parameters used in the model are $T_{cs}=90$ K, zero-temperature penetration depth $\lambda_s(0)=1500$ Å, normal state conductivity $\sigma_s=1.0\times10^6$ $1/\Omega$ m, and thickness $d_s=3000$ Å, while for the normal metal layer $T_{cN}=57$ K, $\sigma_N=4.44\times10^5$ $1/\Omega$ m, and $\lambda_N(0)=5500$ Å. The results of this model, which are shown in Fig. 6, reproduce several important qualitative features of the YPrBCO/YBCO bilayer data. The calculated surface reactance [proportional to $\Delta\lambda_{\mathrm{eff}}(T)$] shows a kink approximately 1 K below T_{cN}, and of course no sign of a drop in $\Delta\lambda_{\mathrm{eff}}(T)$ just above T_{cN}. The calculations also show that the kink becomes more distinct with increasing d_N, just like the data (Fig. 2). The calculated surface resistance shows a nonmonotonic temperature dependence which is similar to the data in Fig. 3 and a monotonic decrease of $T_{\max}$ with increasing d_N, in good agreement with the data. In addition, the increase in $T_{\min}-T_{\max}$ with increasing d_N, the increase in the magnitude of the $R_s(T)$ bump, and the fact that $T_{\min}$ is not a strong function of d_N are also in good qualitative agreement with the data (see Table I). However, the model predicts that bilayers with thicker d_N have a slightly larger $\Delta\lambda(T)$ above T_{cN}, in contradiction with the data, which shows that the 3000-Å YPrBCO/YBCO bilayer has the smallest $\Delta\lambda_{\mathrm{eff}}(T)$ above T_{cN}.

Also note that the model predicts the minimum in $R_s(T)$ always occurs at T_{cN}, whereas the data show minima 3–5 K above T_{cN}. From the inset in Fig. 1, we see that the dc resistance of YPrBCO is a monotonic function of temperature above T_{cN}; hence the increase of $R_s(T)$ above T_{cN} is not simply related to the dc properties. The fact that $T_{\min}$ is nearly independent of d_N suggests that this feature is intrinsic to YPrBCO of this doping level. The minimum of $R_s(T)$ above T_{cN} suggests that the ab-plane conductivity of the YPrBCO layer increases dramatically at that point. This is consistent with a reduction of the quasiparticle scattering rate in YPrBCO above T_{cN}, in agreement with THz spectroscopy measurements on YPrBCO.[31] A softening of the transverse optical phonon modes in the same temperature range above T_{cN} of YPrBCO has also been observed by Raman spectroscopy,[32] suggesting that all of these observations have a common origin, possibly in the opening of a spin gap.

These results are also consistent with the observation of Polturak *et al.* of an increase in I_c of their *S-N-S* device above T_{cN}.[6,21] Finally, it is found from the two-superconductor model that if the YPrBCO layer does not

have a conductivity which increases below T_{cN}, then one does not reproduce a large peak in $R_s(T)$ near T_{cN}.

V. CONCLUSIONS

We find that measurements of the surface impedance of superconductor/normal-metal bilayers give insight into the proximity effect and the electrodynamics of coupled superconductors. The surface impedance data on c-axis YBCO/YPrBCO bilayers are consistent with proximity coupling in the c direction between the two materials with a coherence length $\xi_N(T_{CN}+2\ \mathrm{K}) \lesssim 1$ nm. It is also consistent with the behavior of two isolated superconductors in a bilayer geometry. At least one of the characteristics of proximity coupled superconductors, namely, a strong downturn of the effective penetration depth above T_c, was not observed in the high-T_c bilayer films. This result is consistent with the absence of metallic transport in the c direction in YPrBCO. However, the increase of $R_s(T)$ above T_{cN} is a sign that $\sigma_1(T)$ of the YPrBCO layer is strongly enhanced near T_{cN}, consistent with the rapid reduction of the quasiparticle scattering rate above T_{cN}, and the opening of a spin gap, in that material. Our experiment, although originally designed to investigate the proximity effect, is also a technique to study the normal state electrodynamics properties of thin films which are backed by a higher-T_c superconducting film.

ACKNOWLEDGMENTS

This work was supported by the NSF through Grant Nos. DMR-9123198 and DMR-9624021, and NSF Academic Research Infrastructure Grant No. DMR-9214579.

*Present address: HYPRES Inc., 175 Clearbrook Road, Elmsford, New York 10523.

†Corresponding author, electronic address: anlage@squid.umd.edu.

[1] K. Char, L. Antognazza, and T. H. Geballe, Appl. Phys. Lett. **63**, 2420 (1993).

[2] C.-R. Hu, Phys. Rev. Lett. **72**, 1526 (1994).

[3] M. Sigrist, D. B. Bailey, and R. B. Laughlin, Phys. Rev. Lett. **74**, 3249 (1995).

[4] K. A. Delin and A. W. Kleinsasser, Supercond. Sci. Technol. **9**, 227 (1996).

[5] P. G. de Gennes, Rev. Mod. Phys. **36**, 225 (1964).

[6] E. Polturak *et al.*, Phys. Rev. Lett. **67**, 3038 (1991).

[7] A. W. Kleinsasser and K. A. Delin, Appl. Phys. Lett. **66**, 102 (1995).

[8] K. Char, L. Antognazza, and T. H. Geballe, Appl. Phys. Lett. **65**, 904 (1994).

[9] L. Antognazza *et al.*, Phys. Rev. B **52**, 4559 (1995).

[10] G. Deutscher (private communication).

[11] A. W. Kleinsasser, Appl. Phys. Lett. **66**, 394 (1995); K. Char, L. Antognazza, and T. H. Geballe, *ibid.* **66**, 395 (1995).

[12] M. S. Pambianchi, J. Mao, and S. M. Anlage, Phys. Rev. B **50**, 13 659 (1994).

[13] M. S. Pambianchi, S. N. Mao, and S. M. Anlage, Phys. Rev. B **52**, 4477 (1995).

[14] M. S. Pambianchi, L. Chen, and S. M. Anlage, Phys. Rev. B **54**, 3508 (1996).

[15] A. J. De Marco *et al.* (unpublished).

[16] K. A. Delin and A. W. Kleinsasser, IEEE Trans. Appl. Supercond. **AS-5**, 2976 (1995).

[17] G. Deutscher and R. W. Simon, J. Appl. Phys. **69**, 4137 (1991).

[18] Q. Li *et al.*, Phys. Rev. Lett. **64**, 3086 (1990).

[19] A. Inam *et al.*, Appl. Phys. Lett. **53**, 908 (1988).

[20] C. Kwon *et al.*, Appl. Phys. Lett. **62**, 1289 (1993).

[21] Although Polturak *et al.* (Ref. 6) used a Pr doping which is nominally identical to ours, their T_c was reported to be only 40 K. The authors of that paper report an increase of I_c of 5 K above T_{cN}, and attribute it to the proximity effect, although others (Ref. 7) suggest it is likely caused by inhomogeneous Pr doping.

[22] R. C. Taber, Rev. Sci. Instrum. **61**, 2200 (1990).

[23] B. W. Langley *et al.*, Rev. Sci. Instrum. **62**, 1801 (1991).

[24] M. S. Pambianchi, Ph.D. thesis, University of Maryland, 1995.

[25] The full expression relating Q and R_s is $1/Q = R_s/(\pi\mu_0 f_0 d) + (1/Q_{\mathrm{ff}}) + \tan\delta$, where Q_{ff} is a measure of the energy lost via coupling through the fringing fields at the edges of the resonator, and $\tan\delta$ quantifies the dielectric loss. Weak coupling is assumed, so that any additional term $1/Q_{\mathrm{coupling}}$ may be neglected. Q_{ff} and $\tan\delta$ were determined by varying the thickness of the spacer over the range $12.5\ \mu\mathrm{m} \leqslant d \leqslant 125\ \mu\mathrm{m}$. By fitting d/Q to a quadratic function of d, these extrinsic sources of loss were extracted and accounted for. See Refs. 22 and 24.

[26] M. Pambianchi, S. M. Anlage, E. Hellman, E. Hartford, M. Bruns, and S. Y. Lee, Appl. Phys. Lett. **64**, 244 (1994).

[27] The empirical form for $\lambda(T) = \lambda(0)/[1-(T/T_c)^2]^{1/2}$ was first used for YBCO films by J. M. Pond *et al.*, Appl. Phys. Lett. **59**, 3033 (1991), and is introduced here only to estimate the value of $\lambda(0)$. It is well known that the parallel plate resonator measurement technique does not determine the absolute value of $\lambda(0)$; hence one is forced to use empirical fits such as this to obtain an estimate. In addition, the fit T_c values are not an accurate measure of the transition temperature.

[28] N. Klein *et al.*, J. Appl. Phys. **67**, 6940 (1990).

[29] G. Deutscher, J. P. Hurault, and P. A. van Dalen, J. Phys. Chem. Solids **30**, 509 (1969).

[30] The use of Mattis-Bardeen electrodynamics is for calculational convenience. Mattis-Bardeen has one important feature in common with cuprate electrodynamics, namely, a rapidly rising $\sigma_{1N}(T)$ just below T_{cN} [see, e.g., D. A. Bonn *et al.*, Phys. Rev. Lett. **68**, 2390 (1992)]. Note that the use of a two-fluid $\sigma_1(T)$ alone will not produce the observed large increase in $R_s(T)$ below T_{cN} in the two-superconductor model.

[31] R. Buhleier *et al.*, Phys. Rev. B **50**, 9672 (1994).

[32] A. P. Litvinchuk, C. Thomsen, and M. Cardona, Solid State Commun. **83**, 343 (1992).